PCCP

Accepted Manuscript

ROYAL SOCIETY OF CHEMISTRY

www.rsc.org/pccp

Microsecond molecular dynamics simulation of guanidinium chloride induced unfolding of ubiquitin

Manoj Mandal and Chaitali Mukhopadhyay*

Department of Chemistry, University of Calcutta

92, A.P.C. Road, Kolkata – 700 009, India

Running Title: Guanidinium chloride induced unfolding of ubiquitin.

Address for Correspondence:

Chaitali Mukhopadhyay

Department of Chemistry,

University of Calcutta,

92, A.P.C. Road, Kolkata - 700 009, India

Email : chaitalicu@yahoo.com, cmchem@caluniv.ac.in

Phone : 91-033-2351-8386

FAX : 91-033-2351-9755

ABSTRACT

Atomic detail mechanism of guanidinium induced unfolding of a protein ubiquitin have been explored from all atom molecular dynamics simulation. Ubiquitin unfolds through pre-unfolded (intermediate) states i.e. guanidinium induced unfolding of ubiquitin appears to be a multi-step process and loss of hydrophobic contacts of C-terminal residues are crucial for ubiquitin unfolding. Free-energy landscapes show barrier separation between folded and unfolded basins is ~5.0 Kcal/mol and both the basins are of comparable energy. It was observed that guanidinium ions interact directly with ubiquitin. Favorable electrostatic interaction is the main driving force for such accumulation of guanidinim ions near protein whereas van der Waals energy also contributes. RDF plots show that accumulation of guanidinium ions near specific residues is the main cause for destabilization of intra-residue interactions crucial to maintain the three-dimensional fold of the protein. One salt-bridge interaction between Lys11 and Glu34 appears to be important to maintain the crystal structure of ubiquitin and this salt-bridge can map the unfolding process of ubiquitin.

1. INTRODUCTION

Despite decades of active research there are lacunae existing in the understanding of chemical unfolding of proteins. Though an effective and widely used protein denaturant, much less work has been done for guanidinium chloride (Gdmcl) induced denaturation[1-6] compared to its counterpart urea[3-11]. This requires understanding about the nature of interaction between guanidinium ions and proteins via contact formation i.e. through “direct mechanism” or through an “indirect mechanism” where denaturants disrupt the structure of water and thus enhance the solubility of hydrophobic groups of proteins. Reports supporting either of the mechanisms are available in the literature[5,8,12]. The report suggesting that guanidinium ions do not form hydrogen

bonds with protein backbone[13] is countered by results where guanidinium ions are shown to form hydrogen bonds with protein backbone.[5] Selectivity of guanidinium ions towards backbone and side-chain atoms is also not well established. Which interaction is stronger or are both equally contributing to the unfolding process? Is there any special effect of guanidinium ions on specific residues? Being a charged species can guanidinium ions affect the strength of salt-bridges during the process of unfolding?

To establish a detail structural view of the denaturation mechanism of guanidinium hydrochloride proteins with distinct core is preferable.[8] Ubiquitin, a 76 residue protein with a well-defined hydrophobic core, N and C termini beta sheet are in close contact which is a common characteristic of two-state folders,[14] early investigations reported that ubiquitin is an apparent two state folder[15-18] But later studies proposed that depending upon the experimental[9-28] and simulation[29-31] conditions additional on or off pathway intermediates may be populated. It is known that the C-terminal region of ubiquitin i.e. beta strands III, IV and V are more dynamic i.e. less conformationally stable, compared to the N-terminal region[26] i.e., I and II beta strands and alpha-helix. However, it is unknown whether guanidinium ion can affect the trend and magnitude of the dynamics. To address the above mentioned issues, we performed extensive all atom molecular dynamics simulation of ubiquitin in ~ 6M Gdmcl solution and in pure water [see supporting material (SM)]. We find that denaturation of ubiquitin occurs through several intermediate states and present a probable mechanism of Gdmcl induced denaturation of ubiquitin.

2. METHODS

The simulation was carried out using the program NAMD2.7[32] with CHARMM27force field.[33] TIP3P model[34] of water was used. Guanidinium chloride parameters were taken from reference 35. To prepare the ~6M gdmcl solution of ubiquitin (PDB code: 1UBQ.pdb), ubiquitin molecule was immersed into well equilibrated solution of gdmcl and overlapping solvent molecules were deleted. The final solution contains one ubiquitin molecule in the centre along with 1762 water and 464 guanidinium chloride molecules with a box size of nearly 50.5 Å × 50.5 Å × 50.5 Å. The SHAKE algorithm is used to restrain the covalent bonds containing hydrogen atoms at their equilibrium distances.[36] A nonbonded cutoff of 12 Å was used and the nonbonded list was updated every 20 steps. Periodic boundary conditions and minimum image were used to reduce edge effects. Particle Mesh Ewald(PME) method was applied to calculate the long-range electrostatic interactions.[37] The system was minimized with Steepest Descent and Adopted Basis Newton-Raphson methods. After heating slowly to 300K, the system was equilibrated for 1ns in NPT ensemble followed by more than 1.34 μs production run with 2fs time step in NVT ensemble. The temperature was kept constant through Langevin bath with coupling coefficient τ_T = 0.1 ps. System preparation and trajectory analysis was performed with CHARMM (Chemistry at Harvard Macromolecular Mechanics) and the visual analysis of the trajectories using Visual Molecular Dynamics(VMD).[38] We have performed another independent simulation of ubiquitin in ~6M Gdmcl solution [see supporting material (SM)] and both the results are consistent.

3. RESULTS AND DISCUSSION

Control Simulation:

Control Molecular dynamics simulation of ubiquitin in pure water at 300K was performed for more than 700ns using same force-field and protocol. Visual inspection of the control simulation trajectory did not show any significant structural change throughout the simulation. Results from the analysis (R_g, RMSD, SASA) [see supporting material (SM) for details] of ubiquitin does not show any large change upto ~700ns which confirmed that current force-field can reproduce the solution structure of ubiquitin.

RMSD and R_g plot

Backbone root mean square deviation (RMSD) value is calculated to investigate the time evolution of conformational changes of ubiquitin from its crystal structure. Time vs. RMSD plot shows (Figure 1a) no significant change during first ~ 350ns, after which a sudden increase is observed, followed by large fluctuations. Prior to the sudden change, the conformation with RMSD value ~4.4 Å is comparatively highly populated which may be an indication of pre-folding state of ubiquitin. Radius of gyration(R_g) is another effective measurement and large change in R_g value provides direct evidence about protein unfolding. Time evolution plot of R_g of backbone alpha carbon atoms (shown in Figure 1a) shows large change after ~350ns consistent with RMSD plot. We found a relatively higher populated state at ~12.6Å R_g value. R_g value of backbone alpha carbons of hydrophobic core vs. time plot shows (Figure 1c) similar trend like R_g and RMSD (Details given in SM text).

SASA plot:

Time dependent change in the solvent accessible surface area (SASA) is used to monitor the unfolding process. The plot (Figure 1b) shows ubiquitin starts unfolding after ~350ns when

average SASA value sharply increases from ~5600Å^2 to ~7000Å^2 and it also confirms the existence of intermediate states and follows same trend as R_g and RMSD plots. To account for the contribution of hydrophobic residues in the change of SASA we have calculated SASA for hydrophobic residues separately. These plots show that average SASA value of hydrophobic residues increases from ~4400 Å^2 to ~5400 Å^2 accounting for nearly 75% of the overall change in SASA. This clearly indicates loss of hydrophobic contacts being crucial for unfolding.

Free-energy landscapes

Fraction of Contact vs. RMSD

To map the unfolding pathway two dimensional free-energy landscape was constructed (shown in Figure 2a) from the joint - probability of fraction of contacts (defined as any two Cα atoms which are within 7Å) and RMSD[39-43] using the equation F= -RTlnP where P is the joint-probability. This plot evidently shows folding to unfolding transition through number of stable intermediates or pre-unfolding states. The plot shows that transition from one intermediate state to another go through high energy path. Similar intermediate states have been characterized by several experiments[19-28] and simulations[29-31, 44-46].Free-energy plot shows that the unfolded state basin stability is comparable to folded basin which is the driving force for gdmcl induced ubiquitin unfolding. Free-energy barrier separation from folded basin to unfolded basin is ~5.0-6.0 kcal/mol which is close to the value reported by Chung et al(~7 kcal/mol)[47] and Piana et. al(~5 kcal/mol)[29] for ubiquitin molecule. One fairly populated intermediate state has been observed nearly at Fraction of contact value ~0.85 ± 0.01 and RMSD value ~4.3 ± 0.1 Å. Few other comparatively stable but high energy intermediate states have been observed during unfolding, similar to that reported by Piana et. al.[29] Larios et. al., suggested that lower stability of

intermediate ensemble of guanidinium chloride denaturation of ubiquitin makes it difficult to characterize.[1] We plotted another free-energy surface constructed from R_g and RMSD (shown in supporting information Figure S1). This plot is consistent with above mentioned free-energy surface and confirms all the intermediate states shown. One dimensional free energy plot from RMSD value (shown in Figure S2 in Supporting Material) is closely comparable to the free-energy plot shown by Piana et. al[29], intermediate states along with pre-unfolded state is also clear from this one dimensional free – energy plot.

N-terminal vs. C-terminal part

To distinguish which part of protein is mainly responsible for folding – unfolding transition of ubiquitin, we plotted free-energy landscape of R_g of N-terminal part (residue number 1 to 34)(R_{gN}) vs. C- terminal part (residue number 35 to 76)(R_{gC}). (Shown in Figure 2b)This plot shows two well defined domain, folded domain and unfolded domain separated by comparatively stable intermediate states. This plot shows loosely compact native state, C-terminal part is fluctuating and almost no change for N-terminal part. Larios et. al, suggested that during refolding prior to the native-state formation, ubiquitin forms a compact ensemble with native – like secondary structure without tight packing[1]. We found ensembles with higher R_{gC} value in folded basin which is characterized as pre-unfolded state resulting from loss of compactness of C-terminal part and other states are characterized and shown through arrows. We found two types of unfolded ensembles, one with loose C-terminal part and another with comparatively compact C-terminal part and both cases compactness of N-terminal part largely fluctuates, although more compact structure (where beta-hairpin is close to from alpha-helix) is comparatively highly populated than less compact structure (where beta-hairpin is far from alpha-helix).

Direct interaction between ubiquitin and solvent

Backbone – solvent RDF

To probe the effect of guanidinium ion on the structure of ubiquitin, we have calculated radial distribution functions (RDF) of backbone and side chain atoms of ubiquitin with atoms of guanidinium and water. Two types of backbone RDFs were calculated: one between the carbonyl oxygen(O_B) and hydrogen atoms of guanidinium(H_G) [$g(O_BH_G)$] and water (H_W) [$g(O_BH_W)$]. The other is between the amide hydrogen (H_B) and guanidinium nitrogen(N_G)[[$g(H_BN_G)$] and water oxygen(O_W) [$g(H_BO_W)$]. The RDFs were calculated from the first 20 ns, 410 ns to 430 ns and last 20 ns of the trajectory and shown in (Figure 3a and 3b) respectively. The first peaks of both $g(O_BH_G)$ and $g(O_BH_W)$ are located at ~1.8 Å which is the characteristic peak of hydrogen bonding. While the first peak height of $g(O_BH_G)$ effectively increases from 0.54 to 0.84 an intermediate value of peak intensity ~0.70, the corresponding first peak magnitude(~1.01) of $g(O_BW_H)$ shows marginal decrease from ~1.01 to 0.98. Beyond first peaks, significant increase of other peak intensity of $g(O_BH_G)$ implies accumulation of guanidinium ions near carbonyl oxygen increases whereas no considerable change for others peaks of $g(O_BW_H)$ demonstrate accumulation of water molecule near carbonyl oxygen of ubiquitin remain unchanged. RDF plot from 410ns to 430ns of trajectory shows how guanidinium ions are hydrogen bonded and accumulated near backbone carbonyl oxygen during the process of large scale tertiary contact loss. This preferential binding of guanidinium ions with carbonyl oxygen is one of the key mechanism by which guanidinium ions breaks the backbone – backbone hydrogen bonding of native ubiquitin and consequently unfold ubiquitin from its native state. RDFs between amide hydrogen(H_B) with nitrogen atom of guanidinium(N_G)[$g(H_BN_G)$] shows increased peak height at longer distance indicating higher accumulation of guanidinium ion near backbone amide

hydrogen. RDF plots between backbone amide hydrogen(H_B) and water oxygen(O_W) [$g(H_BO_W)$] shows the hydrogen bonded peak intensity increases from ~0.59 to ~0.75 after unfolding of ubiquitin and also the second peak(~ 5.65 Å) height increases. RDF plots between backbone hydrogen and chloride atom (shown in Figure S5 in SM) shows substantial accumulation of chloride atom around H_B atoms during unfolding.

Side-chain - solvent RDF

To account for the effect of solvent on side-chains we have calculated RDFs between negatively charged side-chain resides (e.g. aspartic acid and glutamic acid) with solvent molecule and shown in Figure 3c) and Figure S6 in SM respectively. Negatively charged side-chain oxygen of aspartic acids (OD) and glutamic acids (OE) are solvated by both H_G and H_W but extent of solvation is much greater by guanidinium ion than water and solvation of glutamic acid oxygen by guanidinium ion is slightly higher than aspartic acid oxygen.

Non-polar residue – solvent RDF

Guanidinium ion induced unfolding of ubiquitin involves loss of hydrophobic interaction as shown in R_g of hydrophobic core and hydrophobic groups. To explore the effect of guanidinium ion to the hydrophobic groups, we have calculated RDF plots between β-carbon of hydrophobic groups and carbon atom of guanidinium ions(shown in Figure 3d). RDF plots show that concentration of guanidinium ion around the hydrophobic group increases adequately for unfolded state than folded state. Intensity of first peak position at ~5.0Å is shifted to closer distance to ~4.9Å and peak intensity increases from 0.51 to 0.67, a new moderately structured second peak is formed at ~6.6Å, third peak intensity at ~10.0Å increases significantly and is shifted to 9.8Å. Shifting of first peak distance to a comparatively shorter distance reflects

augmented interaction strength of guanidinium ion with hydrophobic side-chain. The plot at 410 to 430ns shows that although the concentration of guanidinium ion increases around the hydrophobic groups but broad peak indicates that the guanidinium ions are fluctuating near the hydrophobic groups and try to stabilize the hydrophobic groups. The sharp peak for last 20ns RDF plot confirms the stabilization of hydrophobic group by the guanidinium ions. RDF plots of water oxygen around the β-carbon of hydrophobic side chain show that strong first peak at ~3.6Å as well as the second and third peaks decrease considerably which indicates that density of water molecule near these hydrophobic side-chain decreases.

Fraction of contact

Loss of native contacts is one of primary events associated with unfolding of protein. It also provides information about intermediate states during the process of unfolding. We have calculated the backbone – backbone contact defined as any two Cα atoms which are within 7Å (shown in Figure. 1d). Cα- Cα contact plot shows substantial loss of contacts after ~350 ns of simulation indicating unfolding. Fluctuation in contacts for first few hundreds of nanosecond is mostly due to the loss of loose contacts of C-terminal part. and the large loss in contacts after ~350ns. In fact the huge change is mostly due to the loss of contact of C-terminal part of ubiquitin and another considerable fraction due to loss of contact between first and fifth beta strands. These results are consistent with previous unfolding results of ubiquitin.[48]

Ubiquitin - solvent interaction

Time evolution of intra-protein, protein – guanidinium ions and protein – water hydrogen bond pattern illustrated of how loss of protein-protein H-bonds is compensated by formation of protein – solvent and protein – co-solvent hydrogen bonds. The hydrogen bond is defined as distance (between hydrogen and the acceptor atom) and angle (donor-hydrogen-acceptor) cutoffs are 2.4

Å and 120° respectively. Number of ubiquitin – solvent hydrogen bonds (shown in Figure 4a) increases after ~350ns of simulation which is consistent with time evolution of R_g and RMSD plots. Significant loss of intra-protein hydrogen bonds (shown in Figure 4a)) is observed to occur around ~ 600ns.We have plotted the number of backbone – backbone (bb), backbone – guanidinium ions and backbone-water hydrogen bonds with time and also side chain – side chain (ss), side chain – guanidinium ions and side chain – water hydrogen bonds were calculated with time and shown in Figure 4b). These plots show that the decrease in the number of backbone – backbone hydrogen bonds may be the primary mechanism in case of gdmcl induced unfolding of ubiquitin. Side chain – side chain hydrogen bond plot shows that although the population of such type of hydrogen bond is less than bb hydrogen bonds but it contributes considerably in case of gdmcl induced unfolding, as sudden decrease of this type of hydrogen bond after ~350ns is responsible for loss of native tertiary structure of ubiquitin. The number of backbone – guanidinium ion hydrogen bonds did not increase significantly compared to backbone – water hydrogen bonds. Only guanidinium hydrogen's are involved in hydrogen bonding with backbone carbonyl oxygen atoms, this result is also consistent with RDF plots of backbone hydrogen and guanidinium nitrogen(shown in Figure 3b)). Lim et al.[13] has shown that guanidinium ion does not form hydrogen bond with backbone but we find Gdm^+ ion does not form hydrogen bond with backbone through its nitrogen atom whereas it can form hydrogen bond through its hydrogen atoms. Interestingly we have find out one guanidinium ion is involved in hydrogen bonding with backbone oxygen(O_B) of Ile44(shown in Figure S7 in SM) upto more than 400ns from starting of the simulation. Hydrophilic sidechain – guanidinium ion hydrogen bond shows that large amount of guanidinium ion is involed in such type of hydrogen bonding and in fact increase of such type

hydrogen bonds is primarily liable for loss of sidechain – sidechain hydrogen bond and consequent unfolding of ubiquitin.

Energetic of ubiquitin-solvent interaction

RDF plots shows that number of guanidinium ions around ubiquitin molecule increases for unfolded state compare to folded state whereas number of water molecule slightly decreases. The considerable increase of guanidinium ions in First Solvation Shell (FSS) relative to bulk might be explained from an energetic viewpoint. As reported earlier for urea induced denaturation by Hua et al,[8] we have defined any water oxygen atom or carbon atom of guanidinium ions within 5Å of any protein atoms to be in FSS and bulk is defined when they are as far as 6Å from any protein atoms. A non-bonded cutoff of 12.0Å was applied for energy calculation. The calculated probability density plot of electrostatic and van der Waals (vdW) energy between guanidinium ions and protein molecules for FSS and Bulk (shown in Figure 5a) and 5b)). Probability density plots of protein –water electrostatic and vdW interaction energy are shown in Figure 5c) and 5d)). Electrostatic energy probability plot of guanidinium ions shows a decrease of peak height and most importantly peak is slightly shifted to less favorable higher energy value. This is further reflected from difference of average electrostatic energy [-120.36-(-117.63) = -2.73 kcal/mol] between FSS and bulk which shows that movement of guanidinium ions from FSS to bulk is electrostatically favorable. In case of vdW energy plot, peak height does not change but careful examination shows that plot is shifted toward slightly lower energy value. The difference of average vdW energy for guanidinium ion in FSS and in bulk is – 0.29 kcal/mol [i.e. -0.47 – (-0.18)]. Thus, vdW energy, though not the key factor, also contributes for accumulation of guanidinium ion near protein surface as observed in case of urea induced protein denaturation.[8,9] Electrostatic as well as vdW energy calculation shows that more favorable electrostatic energy is

mainly responsible for accumulation of guanidinium ions around ubiquitin molecule and vdW energy might be partially accountable for such gathering.

We have also calculated such probability density plots of water molecules. Difference of average electrostatic energy +0.10 kcal/mol [i.e. -24.39-(-24.49)] of FSS and bulk as well as average vdW energy difference -0.23 kcal/mol [i.e. 2.16-(-2.39)] [comparable with Hua et. al. (-0.24kcal/mol)[8]] shows relatively little advantage for water molecules to pass to FSS from bulk compared to guanidinium ions.

RMSF

Root mean square fluctuation (RMSF**)** determines flexible regions of a protein. Conformational fluctuations have been recognized to be important for protein function. We have plotted RMSF value of ubiquitin averaged from first and last 50ns of the trajectory and shown in Figure 6. Plot from first 50ns clearly shows that loop regions between first and second beta-sheets and second beta-sheet and alpha-helix were the flexible and rest part of N-terminal region was moderately rigid where as the loop regions between third and fourth beta-sheets, forth beta-sheet and 3_{10}-helix, 3_{10}- helix and fifth beta-sheet were the flexible regions with larger rmsf values. This plot shows that the loop regions of ubiquitin become more flexible in presence of guanidinium ions. Last 50ns plot shows that almost all the residues are highly fluctuating.

Salt Bridge

Ubiquitin consisted of many salt-bridges in its native structure. One important salt-bridge is between Lys11 and Glu34, this slat-bridge is important to maintain the crystal structure of ubiquitin and it sustains the contact between N-terminal beta-sheet with the alpha helix. Kitazawa et. al had recently shown that this salt – bridge is one of the key interaction which

controls conformational fluctuation.[49] To recognize the effect of guanidinium ions on this salt-bridge, we have calculated the distance plot between nitrogen(N) atom of Lys11 and oxygen(OE2) atom Glu34 and plotted in Figure 1e). This plot also shows that large increase in distance between the two atoms occurs after ~350ns of simulation. The first event which destabilizes the N-terminal part is loss of this salt-bridge which is visually analyzed using VMD. Breakage of such an important salt-bridge leads to a less compact structure which allows guanidinium ions to enter into the hydrophobic core of ubiquitin. The trend of this plot is similar like R_g, RMSD and SASA plots which indicate that breaking of this salt-bridge has an important role for ubiquitin unfolding and this salt-bridge can map the unfolding process of ubiquitin.

Unfolding mechanism of ubiquitin

Several experimental studies have reported sequential folding of ubiquitin through formation of a stable core between the strand I–II hairpin and the alpha-helix.[1,50,51] The stability of this N-terminal fragment has been investigated by experiments and MD simulation[46,52] and had shown that residual native like structure in the N-terminal beta-hairpin (1-17) and a low population of α-helical conformation (21- 35) in a denatured ubiquitin act as a folding nucleation sites.

Our results indicate that gdmcl induced unfolding of ubiquitin is not a single step process, rather, the unfolding occurs through loss of crucial interactions with time. First of all, salt-bridge interaction between Lys11 and Glu34 is lost within 15ns of simulation. This is one of the important interactions which make close contact of beta-hairpin with alpha helix of the protein. After loss of this interaction beta-hairpin shifts away from alpha helix and opens a channel for guanidinium ions to insert into the hydrophobic core of ubiquitin. RDF plots of hydrogen atom of gunidinium ions around OE2 atom of Glu34 (shown in Figure 1a)) which is calculated from

first 20-30ns simulation time shows sharp increase of first peak which indicates loss of salt-bridge interaction after 20ns due to significant increase of interaction between Glu34 oxygen and hydrogen atoms of guanidinium ions. RDFs plot of water oxygen (O) molecule around OE2 atom of Glu34 (shown in inset of Figure 7a)) shows water density increases marginally near OE2 atom compared to Gdm^+ ions. RDFs plots between CG atom of Lys11 and carbon atom of guanidinium ions (shown in Figure S8 in SM) shows no significant increase of Gdm^+ ions in 10-20 ns indicating that Lys11-guanidinium ions interaction is not vital for destabilization of this salt-bridge. Kitazawa et al. had shown that though short lived, this salt – bridge is one of the key interaction which controls the conformational fluctuation.[49] Our simulation also confirms that this salt – bridge has short live.

A hydrogen-bond interaction which is important for unfolding as well as different intermediate states is that between backbone oxygen(O) of Ilu36 and amide hydrogen(HH11) of Gln41. This side chain – backbone hydrogen bond is located in the loop region following the alpha-helix. The distance plot between O and HH11 (shown in Figure S9 in SM) shows hydrogen bond gets weakened after ~370ns of simulation due to accumulation of guanidinium ions near Gln41 (shown in Figure S10 in SM) and consequently destabilize the hydrogen bonding. Kitazawa et. al using NMR technique had shown that this hydrogen bond is highly conserved which is another key interaction to maintain the native structure of Ubiquitin.[49]

Next important interaction is the hydrogen bonding interaction between carbonyl oxygen atom of His68 and backbone amide hydrogen of Ile44. This hydrogen bond is mainly responsible to maintain the beta-structure of last part of forth beta sheet and contact between last parts of forth beta sheet and first part of fifth beta sheet. This hydrogen bond breaks after 370ns of simulation which is confirmed from RDF plots between CG atom of His68 and carbon atom of guanidinium

ions.(shown in Figure 7d)) This plot shows significant increase of first peak and solvent separated second peak after 380ns compared to 320ns, further increases as of guanidinium ions near CG atom confirmed from RDF plot of last 20ns. RDF plot of water oxygen around CG atom of His68 (shown in inset of Figure 7d)) shows density of water molecule around His68 decreases significantly.

Just after the destabilization of this hydrogen bond, another between carbonyl oxygen atom of Arg42 and backbone amide hydrogen of Val70 residue gets weaker which cracks the fifth beta-sheet into two smaller units. This hydrogen bond is important because we observed that this state behave as a pre-unfolded state. RDF plots between CG atom of guanidinium group of Arg42 and carbon atom of guanidinium ions (shown in Figure 7b)) shows accumulation of guanidinium ions starts after 370ns of simulation and larger accumulation was observed for last 20ns. We found two types of accumulation namely stacked (~3.8-3.9Å) and solvent separated (~7.6-7.8Å) which were also observed in our previous work where we found similar types guanidinium ion pairing[53] and also from other reports.[54,55] RDFs shows that after ~370ns density of both stacked and solvent separated form also increases significantly i.e. Arg42 gets solvated by guanidinium ions which are responsible for destabilization of this hydrogen-bond. RDFs plot of guanidinium carbon (C_G) around beta carbon of Val70 (CB_{V70}) (shown in Figure S11 in SM) shows increase of guanidinium ions around Val70 after 370ns of simulation.

Subsequently another important hydrogen bond gets weaker in between backbone amide hydrogen of Lys6 and carbonyl oxygen of Leu67 residues, which maintain the contact between first and fifth beta-hairpin, this contact gets destabilized after ~400ns of simulation. The most important hydrogen bond that maintains the contact between first beta-sheet and fifth beta sheet is that between amide hydrogen of Leu67 residue and carbonyl oxygen of Phe4 residue. This

hydrogen bond persists after loss of fifth beta sheet. After ~400ns guanidinium ions try to accumulate near the Leu67 residue which weaken the hydrogen bond between amide hydrogen of Lys6 and carbonyl oxygen of Leu67 residues and larger accumulation after ~460ns shown from RDF plots of guanidinium carbon(C_G) around CG atom of Leu67 (Figure 7c)) and peak shifts towards shorter distance confirms the superior interaction between Leu67 and Gdm^+ ions which destabilize this hydrogen bond, after which beta hairpin gets detached from fifth beta residues and ubiquitin unfolds. Our mechanism is consistent with several experimental results.[25,27]

From these plots it is obvious that accumulation of Gdm^+ ions near both hydrophilic and hydrophobic residues are responsible for destabilization of favorable interaction involving that residue and gradually unfolding. Guanidinium ion form stacked with aromatic rings and guanidinium part of arginine due to its aromatic, hydrophobic character[56,57] and favorable aromatic – aromatic interactions.[58,59] Beta hairpin follows the sliding mechanism during unfolding, it slides around the hydrophobic faces of fifth beta reside and unfolds.

Contact map

Cross correlation map of alpha carbon atoms provides clear picture of protein skeleton through contact information. Cross correlation map constructed at different time points can represent actual mechanism of protein unfolding by showing which contacts are lost or misplaced and which are formed. The contact composition is largely made up of hydrophobic and polar residues, although few crucial aromatic, acidic and basic residues can be involved.[60] A contact is defined if alpha carbon atoms are within 7.0 Å. The structures have been averaged over 5-10ns time frames along the trajectory and plotted in Figure7. The contact map shows loss of contact

between fourth and fifth beta sheet, first and fifth beta sheet and alpha helix region and 3_{10} – helix region which are intermediate states. Contacts between first and fifth beta sheet are lost completely after 450ns whereas few other non-native contacts form between third and fifth beta strands.

Two distinct unfolded states have been characterized through contact map analysis, one when beta hairpin is in close to C-terminal part of protein and other when beta hairpin is far from rest of protein. Both are also combination of two distinct states: one in which beta hairpin is fully structured and other in which beta hairpin is partially unstructured, although partially structured beta hairpin is comparatively less populated than its fully structured form. This result is consistent with experimental studies of urea induced denatured state of ubiquitin which shows N-terminal hairpin forms a considerable amount of residual structure consistent with previous reports [46,52]. We observed hydrophobic patches between Ile44, Val70 and hydrophobic chain and hydrophobic face of guanidine group of Arg42 whereas hydrophobic contacts between Ile44, Val70 were confirmed by previous studies.[61]

Guanidine ion intrusion pathway to His68

From visual inspection we observed the movement of guanidinium ions towards hydrophobic residues of third and forth beta strand. One particular Gdm^+ ion comes closer and interacts with guanidinium group of Arg74, then Gdm^+ ion moves through hydrophobic face of Arg74 side-chain to make hydrogen bond with O_B of Arg74. It then shifts to O_B of Leu73 and moves toward hydrophobic side-chain of Arg72 and again comes toward backbone to from H-bond to O_B of Arg72, from where the Gdm^+ ion jumps to the hydrophobic face of Val70, then to hydrophobic face of Ile42 and hydrophobic side-chain of Arg42 and again comes to Val70. From Val70, it jumps close to His68 ring to form hydrogen bond with NE2 atom and followed by stacking with

His68 ring. This stacking lasted for 2ns and lead to the loss of crucial hydrogen bonding interaction between carbonyl oxygen atom of His68 and backbone amide hydrogen of Ile44. We have drawn a cartoon structure of insertion pathway of Gdm^+ ion towards hydrophobic faces of His68 ring using one pdb structure generated from trajectory (shown in Figure 9).

Comparison for mechanism of action between urea and guanidinium ion induced protein denaturation:

Our present work and previous reported unfolding works with guanidinium chloride (5) and urea(5,8,10) clearly distinguish the mechanism of action for protein unfolding by these two denaturants. Very recent work by Candotti et al. (62) shows urea does not preferentially solvate any residue but binds to the backbone during the first stages of unfolding. They considered that the sticky nature of urea and its preferential placement at hinge points is crucial for unfolding. Urea actively favors unfolding by stabilizing partially unfolded microstates, slowly driving the protein conformational ensemble far from the native one. In one of the earliest papers on urea unfolding by Tirado-Rives et al. (63) it was reported that urea promotes protein unfolding through the stabilization of the unfolded form rather than destabilizing the native state. This is achieved through stabilizing hydrophobic residues that become exposed to solvent upon unfolding. Few other brilliant works from Grubmuller group (64, 65, 66) try to find out whether hydrophobic, or polar interactions are the dominant driving force. Particularly strong preference for contacts to urea were observed for aromatic and apolar side-chains, as well as for the protein backbone, interactions with less polar parts rather than polar interactions are the main driving force for urea induced protein denaturation whereas polar and particularly charged residues had

stronger preferences for interaction with water. Hua et al. (8) and Candotti et al. (10) shows vdW energy is mainly responsible for accumulation of urea molecule near protein molecule.

Present simulation shows favorable electrostatic interaction is the main driving force for accumulation of guanidinim ions near protein. Guanidinium ions solvate the negatively charged side chain residues and initiates the process of unfolding through weakening the charge – charge interactions (salt-bridge) which are responsible for maintenance of the three-dimentional structure of proteins. Hydrophilic sidechain – guanidinium ion hydrogen bond shows that large amount of guanidinium ion is involed in such type of hydrogen bonding and in fact increase of such type hydrogen bonds is primarily liable for loss of sidechain – sidechain hydrogen bonds and consequent unfolding of ubiquitin. Preferential binding of guanidinium ions with carbonyl oxygen is secondary mechanism by which guanidinium ions breaks the backbone – backbone hydrogen bonding of partially unfolded ubiquitin and consequently unfold ubiquitin from its native state and intermediate states. RDF plots show that concentration of guanidinium ion around the hydrophobic group increases adequately for unfolded state than folded state which stabilizes the partially unfolded state like urea molecule and gradually driving the protein conformational ensemble far from the native one.

A recent work done by Koishi et al. (67) shown that Gdm^+ binds with both hydrophobic and hydrophilic faces more favorably compared to urea which is the cause behind effectiveness of guanidinium ions in compare to urea molecule for protein unfolding and stabilizing the hydrophobic residues in partially unfolded states. O'Brien et al. (5) suggested that the superior direct interaction of Gdm^+ with charged species compared to that of urea explains the enhanced efficiency of denaturation of proteins by GdmCl compared to urea and the primary mechanism of denaturation involves direct electrostatic interaction between the denaturant molecules and

proteins. Probably due to the fact, Candiotti et al. (10) found little unfolding on similar proteins after microsecond simulations in urea compare to present simulations with Gdmcl.

4. CONCLUSION

We have characterized guanidinium ion induced pre-unfolding state and intermediate states of ubiquitin from all atom molecular dynamics simulation. Computer simulations can provide critical information on the unfolded ensembles of proteins,[68] from the current simulations we have detected those states and also analyzed the complete unfolding pathway in terms of solute–solvent interaction. Pre-unfolding state of ubiquitin has been characterized from this unfolding simulation which is also reported from various experiments.

Distribution of guanidinium ions around backbone, hydrophobic groups and negatively charged residues determines the destabilization process of ubiquitin. RDFs show Gdm^+ ion forms hydrogen bonding to backbone oxygen atom through its hydrogen atom but did not form with amide hydrogen which may be due delocalized positive charge of guanidinium ion which makes guanidinium nitrogen less basic to form a hydrogen bond to backbone amide hydrogen. RDF plots show guanidinium ions strongly solvate negatively charged residues which affects salt-bridge stability leading to loss of tertiary contacts. Hydrophobic residues are gradually exposed and solvated mainly through hydrophobic faces of guanidinium ions.

Our results confirm the like-charge ion pairing between guanidinium ions and guanidinium group of arginine residues. Important contacts are identified which are responsible to maintain the native structure of ubiquitin and important to map the unfolding process. A plausible mechanism of guanidinium ion intrusion into the hydrophobic core has been sketched.

Ultimately, our results are consistent with reported experimental observations and may promote further studies based on our findings.

5. SUPPORTING MATERIAL

Details of another independent Molecular dynamics simulation of ubiquitin in ~6M Gdmcl and in pure water. Free energy landscape constructed from R_g and RMSD, one dimensional free energy plot constructed from RMSD values, Rg and RMSD plot for another independent simulation, RMSD, R_g, SASA and salt-bridge distance between nitrogen(N) atom of Lys11 and oxygen(OE2) atom Glu34 for ubiquitin – pure water system, definition of hydrophobic core and about time evolution plot of hydrophobic core, Radial distribution functions between backbone hydrogen atom (H_B) of ubiquitin and chloride ions, Radial distribution functions between acidic oxygen (OE2) atom of Glutamic acids (O_E) and guanidiniums hydrogen atom (H_G) and water hydrogen (H_W), The distance plot between backbone oxygen(O) of Ile44 and carbon atom of one specific guanidinium ion, Radial distribution functions between CG atom of Lys11 (CG_{K11}) and guanidiniums carbon atom (C_G) and water oxygen (O_W), The hydrogen bond distance plot between backbone oxygen(O) of Ilu36 and amide hydrogen(HH11) of Gln41, Radial distribution functions between OE1 atom of Gln41 ($OE1_{Q41}$) and guanidiniums carbon atom (C_G) and water oxygen (O_W), Radial distribution functions between CB atom of Val70 (CB_{V70}) and guanidiniums carbon atom (C_G) and water oxygen (O_W).

6. ACKNOWLEDGEMENTS

This work acknowledges financial support of Department of Science and Technology (DST), India (No. SR/S1/PC-60/2009 dt 21/06/2010) for fellowship and computer facility. We also acknowledge UPE of University of Calcutta, for computer facility.

7. REFERENCES

1. E. Larios, S. J. Li, K. Schulten, H. Kihara, and M. Gruebele, J. Mol. Biol. **340**, 115 (2004).
2. J. Ervin, E. Larios, S. Osvath, K. Schulten, and M. Gruebele, Biophysical J. **83**, 473 (2002).
3. M. M. Santoro, and D. W. Bolen, Biochemistry. **27**, 8063 (1988).
4. A. Moglich, F. Krieger, and T. Kiefhaber, J. Mol. Biol. **345**, 153 (2005).
5. E. O'Brien, R. Dima, B. Brooks, and D. Thirumalai. J. Am. Chem. Soc. **129**, 7346 (2007).
6. C. Camilloni, A. Guerini Rocco, I. Eberini, E. Gianazza, R. A. Broglia, and G. Tiana, Biophysical J. **94**, 4654 (2008).
7. Caflisch, A., and M. Karplus. Structure. **7**,477 (1999).
8. L. Hua, R. Zhou, D. Thirumalai, and B. J. Berne, Proc. Natl. Acad. Sci. U.S.A. **105**, 16928 (2008).
9. D. R. Canchi, D. Paschek, and A. E. Garcia, J. Am. Chem. Soc. **132**, 2338 (2010).
10. M. Candotti, S. E. Martin, X. Salvatellaa, and M. Orozoco, Proc. Natl. Acad. Sci. U.S.A. **110**, 5933 (2013).
11. A. Das, and C. Mukhopadhyay, J. Phys. Chem. B. **113**, 12816 (2009).
12. J. N. Scott, N. V. Nucci, and J. M. Vanderkooi, J. Phys. Chem. A. **112**, 10939 (2008).
13. W. L. Lim, J. Rosgen, and S. W. Englander, Proc. Natl. Acad. Sci. U.S.A. **106**, 2595 (2008).
14. M. M. Krishna, S. W. Englander, Proc. Natl. Acad. Sci. U.S.A. **102**, 1053 (2005).

15. T. Sivaraman, C. B. Arrington, and A. D. Robertson, Nat. Struct. Biol. **8**, 331 (2001).

16. M. S. Briggs, and H. Roder, Proc. Natl. Acad. Sci. U.S.A. **89**, 2017 (1992).

17. S. T. Gladwin, and P. A. Evans, Fold Des. **1**, 407 (1996).

18. B. A. Krantz, and T. R. Sosnick, Biochemistry. **39**, 11696 (2000).

19. P. Schanda, V. Forge, and B. Brutscher, Proc. Natl. Acad. Sci. U.S.A. **104**, 11357 (2007).

20. C. R. Babu, V. J. Hilser, and A. J. Wand, Nat. Struct.Mol. Biol. **11**, 352 (2004).

21. F. Cordier, and S. Grzesiek, J. Mol. Biol. **317**, 739 (2002).

22. S. Khorasanizadeh, I. D. Peters, and H. Roder, Nat. Struct. Biol. **3**, 193 (1996).

23. R. Kitahara, and K. Akasaka, Proc. Natl. Acad. Sci. U.S.A. **100**, 3167 (2003).

24. B. Brutscher, R. Bruschweiler, and R. R Ernst, Biochemistry. **36**, 13043 (1997).

25. H. S. Chung, A. Shandiz, T. R. Sosnick, and A. Tokmakoff, Biochemistry. **57**,13870 (2008).

26. A. Vallee-Belisle, and S. W. Michnick, Nat. Struct. Mol. Biol. **19**, 731 (2012).

27. H. S. Chung, M. Khalil, A. W. Smith, and A Tokmakoff, Proc. Natl. Acad. Sci. U.S.A. **102**, 612 (2005).

28. B. A. Krantz, R. S. Dothager, and T. R. Sosnick. J. Mol. Biol. **337**, 463 (2004).

29. S. Piana, K. L. Larson,and D. E. Shaw, Proc. Natl. Acad. Sci. U.S.A. **110**, 5915 (2013).

30. A. Irback, S. Mitternacht, and S. Mohanty. Proc. Natl. Acad. Sci. U.S.A. **102**, 13427 (2005).

31. A. Irback, and S. Mitternacht. Prot. Stuc. Func. and Bio. **65**, 759 (2006).

32. E. Villa, C. Chipot, R. D. Skeel, L. Kale, and K. Schulten, J. Comput. Chem. **26**, 1781 (2005).

33. N. Foloppe, L. Nilsson, and A. D. MacKerell Jr, Biopolymer. **61**, 61 (2001).

34. W. L. Jorgensen, J. Chandrasekhar, J. D. Madura, R. W. Impey, and M. L. Klein, J. Chem. Phys. **79**, 926 (1983).

35. P. E. Mason, G. W. Neilson, J. E . Enderby, M. L. Saboungi, C. E. Dempsey, A. D. MacKerell, and J. Brady, J. Am. Chem. Soc. **126**, 11462 (2004).

36. J. P. Ryckaert, G. Ciccotti, and H. J. C. Berendsen, J. Comput. Phys. **23**, 327 (1977).

37. W. L. Jorgensen, D. S. Maxwell, and J. T. Rives, J. Am. Chem. Soc. **118**, 11225 (1996).

38. W. Humphrey, A. Dalk, and K. Schulten, J. Mol. Graph. **14**, 33 (1996).

39. Y. Liu, J. Strumpfer, P. L. Freddolino, M. Gruebele, and K. Schulten, J. Phys. Chem. Lett. **3**, 1117 (2012).

40. A. Dhar, A. Samiotakis, S. Ebbinghaus, L. Nienhaus, D. Homouz, M. Gruebele, and M. S. Cheung, Proc. Natl. Acad. Sci. U.S.A. **107**, 17586 (2010).

41. Z. Zhuang, A. I. Jewett, S. Kuttimalai, G. Bellesia, S. Gnanakaran, and J. E. Shea, Biophysical J. **100**, 1306 (2011).

42. E. K. Peter, and J. E. Shea, Phys. Chem. Chem. Phys. DOI: 10.1039/c3cp55251a (2014).

43. R. Harada, N. Tochio, T. Kigawa, Y. Sugita, and M. Feig, J. Am. Chem. Soc. **135**, 3696 (2013).

44. S. G. Dastidar, and C. Mukhopadhyay, Phys. Rev. E. **72**, 051928-1 (2005).

45. A. Das, and C. Mukhopadhyay, J. Chem. Phys. **127**, 165103-1 (2007).

46. D. V. O. Alonso, and V Daggett, J. Mol. Biol. **247**, 501 (1995).

47. H. S. Chung, and A. Tokmakoff, Prot. Stuc. Func. and Bio. **72**, 474 (2008).

48. B. J. Stockman, A. Euvrard, and T. A. Scahill, J. Biomol. NMR. **3**, 285 (1993).

49. S. Kitazawa, T. Kameda, M. Y. Utsumi, K. Sugase, N. J. Baxter, K. Kato, M. P. Williamson, and R. Kitahara, Biochemistry. **52**, 1874 (2013).

50. T. R. Sosnick, R. S. Dothager, and B. A. Krantz, Proc. Natl. Acad. Sci. U.S.A. **101**, 17377 (2004).

51. H. M. Went, and S. E. Jackson, Protein Eng Des Sel.**18**, 229 (2005).

52. M. Jourdan, and M. S. Searle, Biochemistry. **39**, 12355 (2000).

53. M. Mandal, and C. Mukhopadhyay. Phys. Rev. E. **88**, 052708-1 (2013).

54. Z. Wu, Q. Cui, and A. Yethiraj, J. Phys. Chem. B. **117**, 12145 (2013).

55. D. Lee, J. Lee, and C. Seok. Phys. Chem. Chem. Phys. **15**, 5844 (2013).

56. M. Vazder, F. Uhlig, and P. Jungwirth,. J. Phys. Chem. Lett. **3**, 2021 (2012).

57. T. Koishi, K. Yasuoka, S. Y. Willow, S. Fujikawa, and X. C. Zeng, J. Chem. Theo. Comp. **9**, 2540 (2013).

58. M. P. D. Hatfiled, R. F. Murphy, and S. Lovas, J. Phys. Chem. B. **114**, 3028 (2010).

59. M. P. D. Hatfiled, R. F. Murphy, S. Lovas, J. Phys. Chem. B. **115**, 4971 (2011).

60. A. Ghose, K. V. Bindra, and S. Vishveshwara, Biophysical J. **92**, 2523 (2007).

61. J. H. Peters, and B. L. Groot, PLOS Comp. Bio. **8**, e1002704 (2012).

62. M. Candotti, A. P. Rez, C. F. Costa, M. Rueda, T. Meyer, J. L. Gelpı, and M Orozco. PLOS Comp. Bio. **9**, e1003393 (2013).

63. J. T. Rives, M. Orozco, W. L. Jorgensen, Biochemistry *36,* 7313-7329 (1997).

64. M. C. Stumpe, H. Grubmuller, Biophysical Journal 96 3744–3752 (2009).

65. M. C. Stumpe, and H. Grubmuller, J. AM. CHEM. SOC. 129, 16126-16131(2007).

66. M. C. Stumpe, and H. Grubmuller, PLOS Comp. Bio. 4 , e1000221 (2008).

67. T. Koishi, K. Yasuoka, S. Y. Willow, S. Fujikawa, and X. C. Zeng, J. Chem. Theory Comput., 9, 2540−2551 (2013).

68. A. Das, B. K. Sin, A. R. Mohazab, and S. S. Plotkin. J. Chem. Phys. **139**, 121925-1 (2013).

Figure Legends

FIG. 1. Time evolution plot of a) RMSD(black) and R_g (red) where F, F_P, I_I, I_{II}, I_{III}, U_I, U_{II}, U_{III} (folded, pre-unfolded, first intermediate, second intermediate, third intermediate, collapsed unfolded, unfolded and largely exposed unfolded states) are shown through black ellipses and ensemble structure of those states are shown in right side with crystal structure of Ubiquitin, named as C. b) Solvent Accusable Surface Area (SASA) of ubiquitin (black) and hydrophobic resides (red) c) R_g of hydrophobic core d) Frction of contact and e) salt-bridge distance between N atom of Lys11 and OE2 atom of Glu34 where inset figure shows distance for first 25ns and representative ensemble structures are shown through ellipses as a, b, c, d, e which are shown in right-side where Lys11 and Glu34 residues are shown in green and orange color respectively.

FIG. 2. Free-energy landscapes constructed from a) Fraction of contact (Y-axix) vs RMSD (X-axix) and b) R_g of C-terminal part(R_{gC}) [Y-axix] and R_g of N-terminal part(R_{gN}) [X-axix]. Both cases above mentioned (fig.1) states are shown through arrows. The color is scaled by Kcal/mol and shown in right-side.

FIG. 3. Radial distribution functions between a) backbone oxygen atom (O_B) of ubiquitin and guanidinium hydrogen atom (H_G) where in inset backbone oxygen atom (O_B) of ubiquitin and water hydrogen atom (H_W) b) backbone hydrogen atom (H_B) of ubiquitin and guanidinium

nitrogen atom (N_G) where in inset backbone hydrogen atom (H_B) of ubiquitin and water oxygen atom(O_W) c) acidic oxygen(OD2) atom of aspertic acids (O_D) and guanidinium hydrogen atom (H_G) where in inset acidic oxygen(OD2) atom of aspartic acids (O_D) and water oxygen(H_W) d) CB atom hydrophobic residues(CB_{pho}) and carbon atom of guanidinium ions(C_G) where in inset CB atom hydrophobic residues(CB_{pho}) and water oxygen(O_W). Black solid line, red dash line and green dotted line represents plot from first 20ns, 410 to 430ns and last 20ns of simulation.

FIG. 4. Number of hydrogen bond between a) backbone atoms of ubiquitin and guanidinium ions (black), water(red) and backbone(green). b) side-chain atoms of ubiquitin and guanidinium ions (black), water(red) and side-chain(green).

FIG. 5. Probability density of a) Electrostatic interaction energy of ubiquitin and guanidinium ions in FSS (black) and Bulk (red) b) van der Walls interaction energy of ubiquitin and guanidinium ions in FSS (black) and Bulk (red) c) Electrostatic interaction energy of ubiquitin and water in FSS (black) and Bulk (red) and d) van der Walls interaction energy of ubiquitin and guanidinium ions in FSS (black) and Bulk (red).

FIG. 6. Root mean square fluctuation of ubiquitin residues vs. residue number from first 50 ns(black rectangle) and last 50ns(red circle). The native secondary structure of ubiquitin is presented at the top of the graph where color scheme for beta strand, alpha helix, 3_{10}- helix and random coil are dark-red(right arrow), red(rounded rectangular), red(small rounded rectangular) and gray.

FIG. 7. Radial distribution functions between a) acidic oxygen atom (OE2) of Glu34 (O_{E34}) and guanidinium hydrogen (H_G) where inset shows acidic oxygen atom (OE2) of Glu34 (O_{E34}) and water hydrogen (H_W) b) carbon atom guanidinium group of Arg42 residue (CZ_{R42}) and

guanidinium carbon atoms(C_G) whereas inset shows carbon atom guanidinium group of Arg42 residue (CZ_{R42}) and water oxygen(O_W). c) CG atom of Leu67 (CG_{L67}) and guanidinium carbon atoms (C_G) whereas inset shows CG atom of Leu67 (CG_{L67}) and water oxygen (O_W). d) CG atom of His68 (CG_{H68}) and guanidinium carbon atoms (C_G) whereas inset shows CG atom of His68 (CG_{H68}) and water oxygen (O_W). For a) solid black line, red dash line, green dotted line and blue dash-dotted line shows plot for first 5ns, 20-30ns, 370-380ns and last 20ns respectively. For b) solid black line, red dash line, green dotted line and blue dash-dotted line shows plot for first 20ns, 300-320ns, 370-380ns and last 20ns respectively. For c) solid black line, red dash line and green dotted line shows plot for first 300-320ns, 370-380ns and last 20ns respectively. For d) solid black line, red dash line and green dotted line shows plot for first 300-320ns, 380-400ns and last 20ns respectively. Representative snapshots show how guanidinium ions (blue) oriented around Phe4(purple), Lys6(orange), Leu8(magenta), Arg42(red), Ile44(gray), Leu67(violet), His68(yellow) and Leu70(tan) residues during folded(I), intermediates(II,III,IV) and unfolded(V) states where β_I, β_{III}, β_V represents first, third and fifth beta strand. These pictures show how guanidinium ions stack with guanidinium part of arginine, phenyl allanine aromatic ring, histidine ring, side chain of arginine and lysine and itself, how it form hydrogen bond with histidine ring nitrogen and backbone oxygen and how it accumulate near hydrophobic residues like leucine, Isoleucine and valine.

FIG. 8. Contact map constructed from backbone Cα atom of ubiquitin averaged over a) first 50ns b) 370 - 380ns c) 395 – 400ns d) 480 – 500ns e) 740 – 750ns f) 940 – 950ns.

FIG. 9. Representative cartoon structure of guanidinium ion intrusion pathway to His68 aromatic ring taken from trajectory snapshot where Lys6(orange), Arg42(red), Ile44(gray), His68(green), Val70(tan), Arg72(lime), Leu73(ochre) and Arg74(purple) residues and

guanidinium ion(blue) stacked with His68 ring are highlighted. Red circle and curved red arrows represents position and pathway of intrusion.

Figures

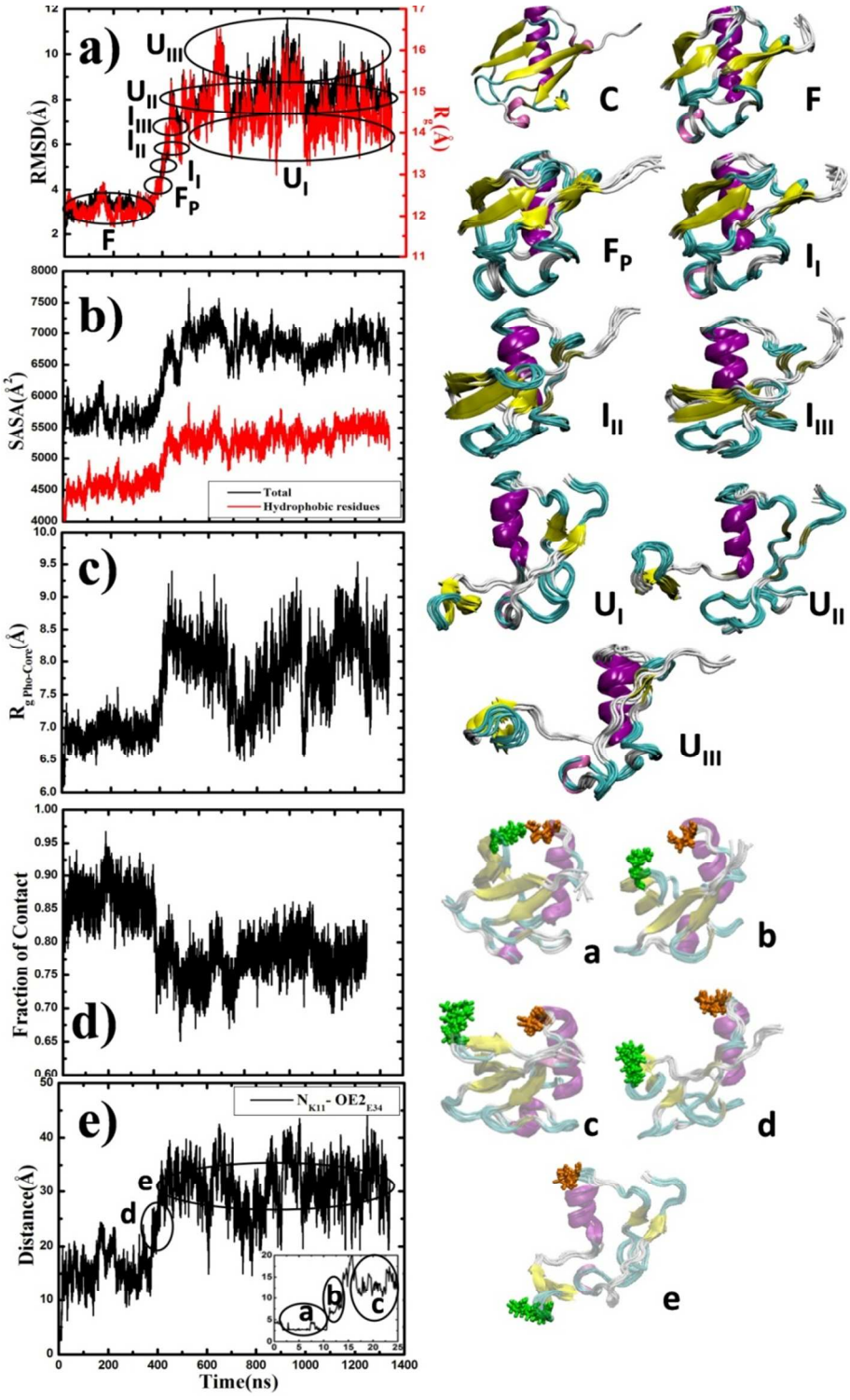

FIG. 1.

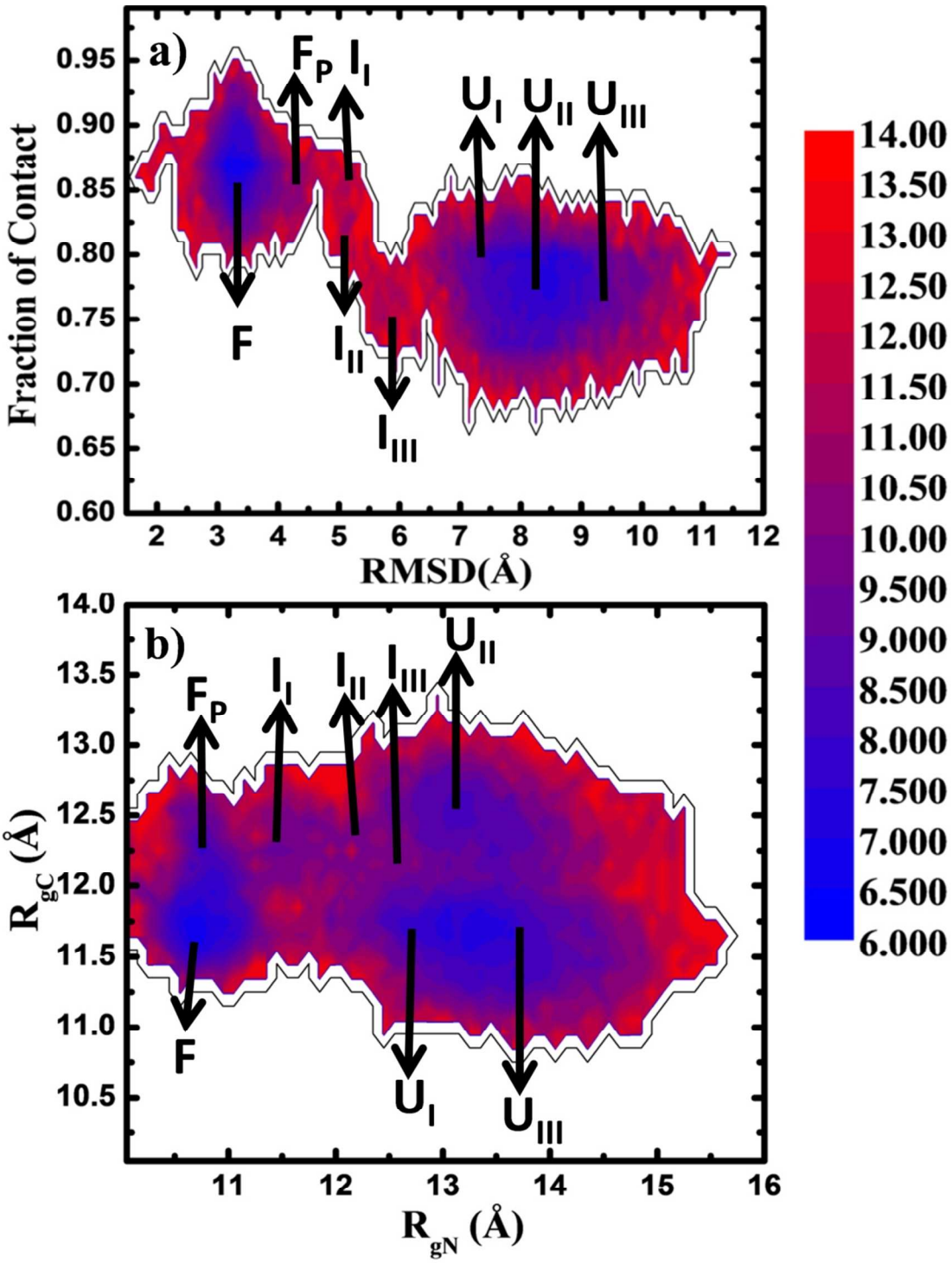

FIG. 2.

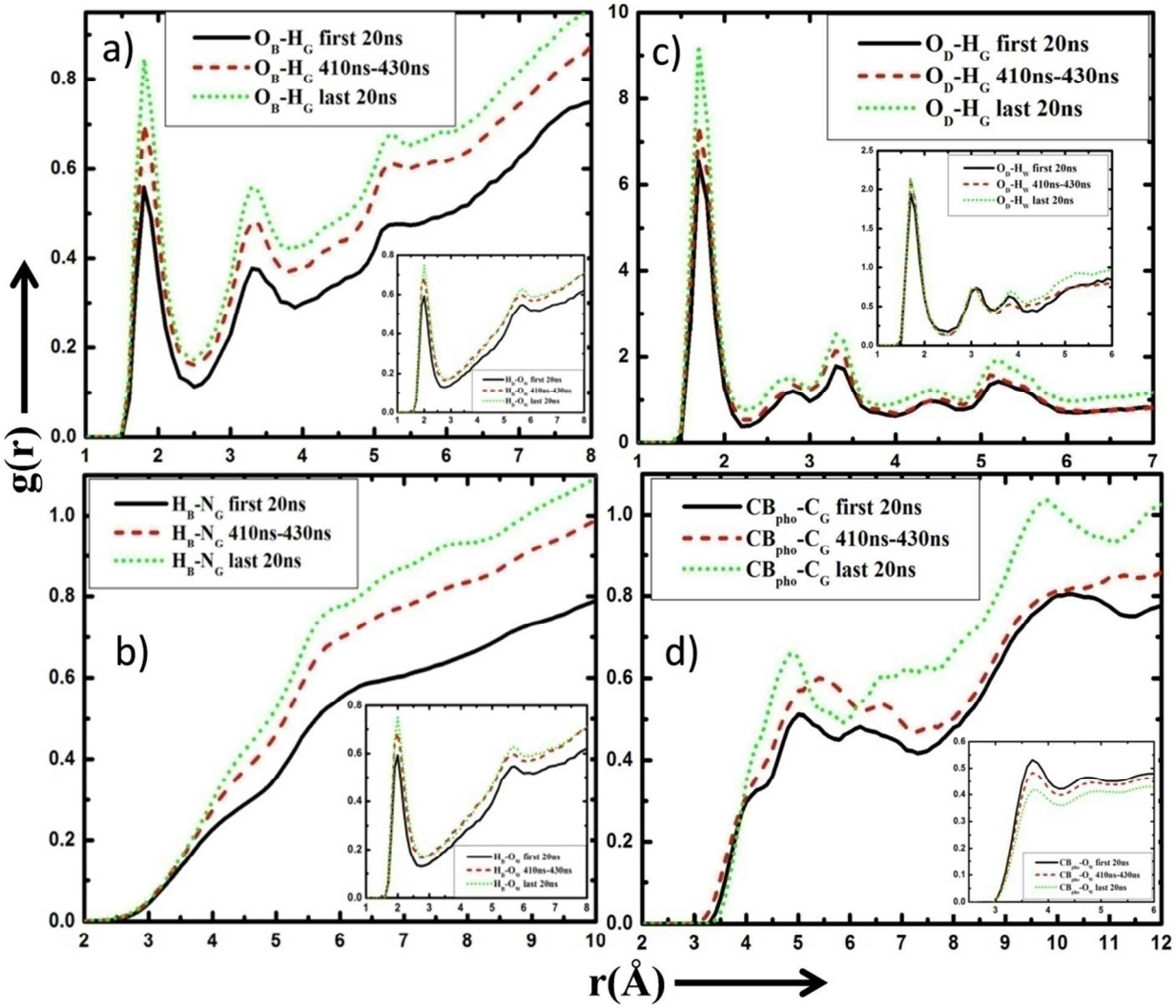

FIG. 3.

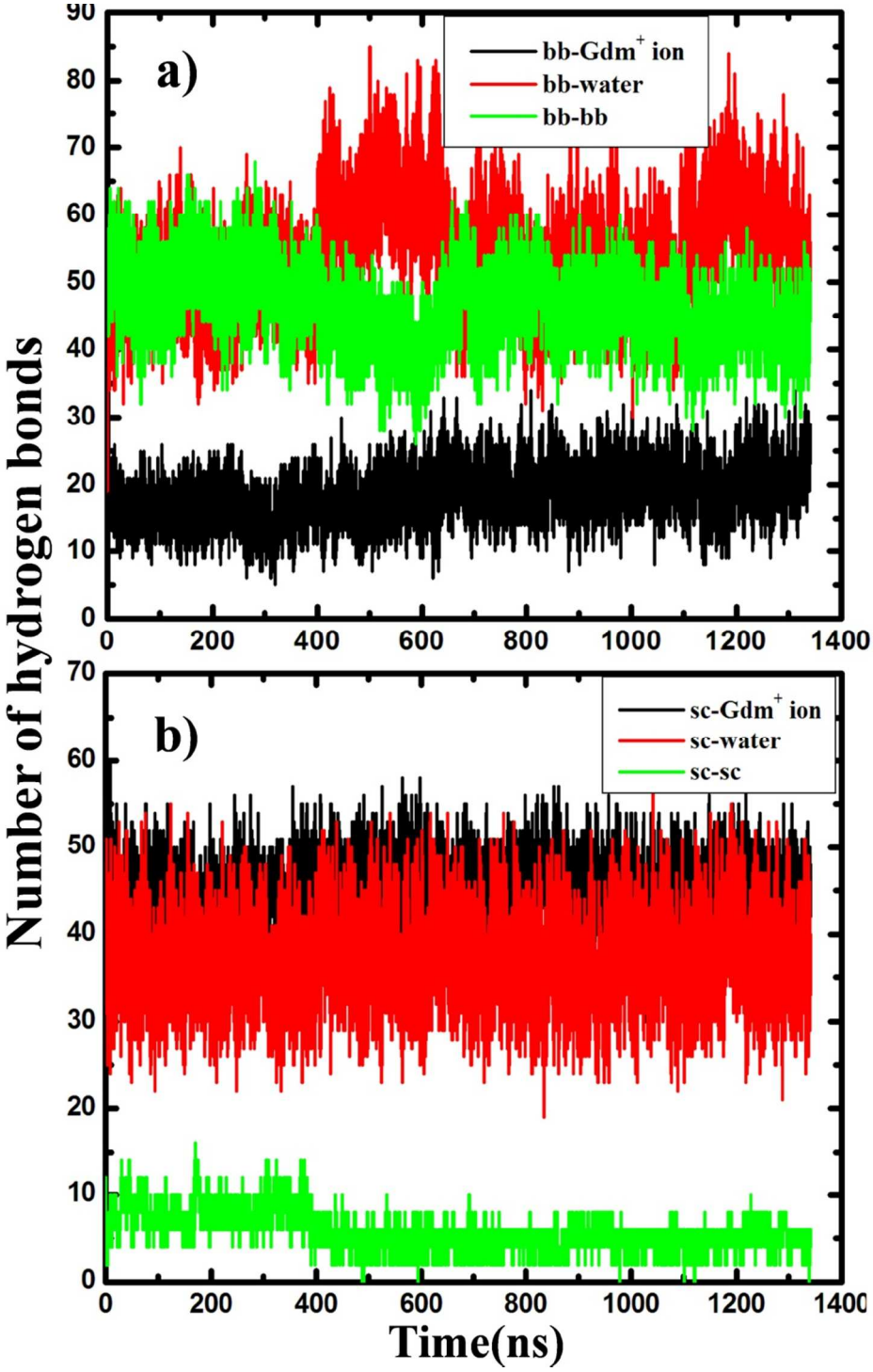

FIG. 4.

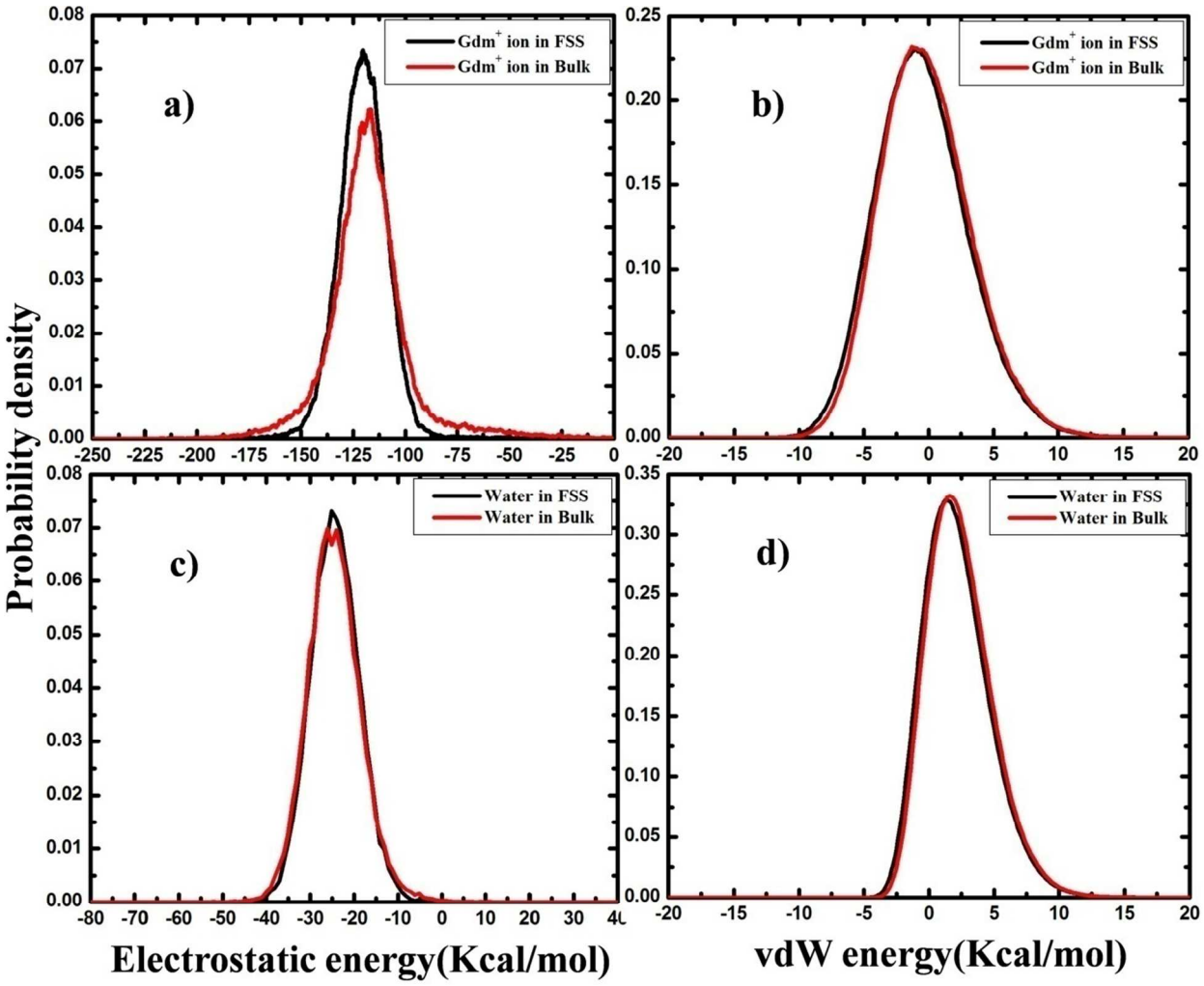

FIG. 5.

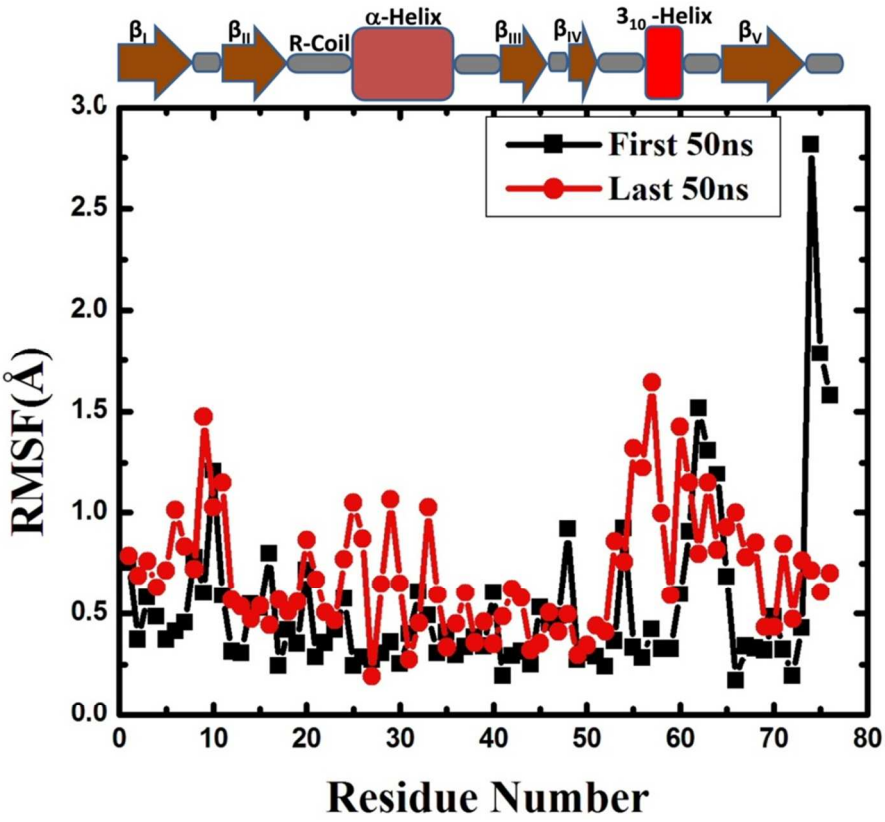

FIG. 6.

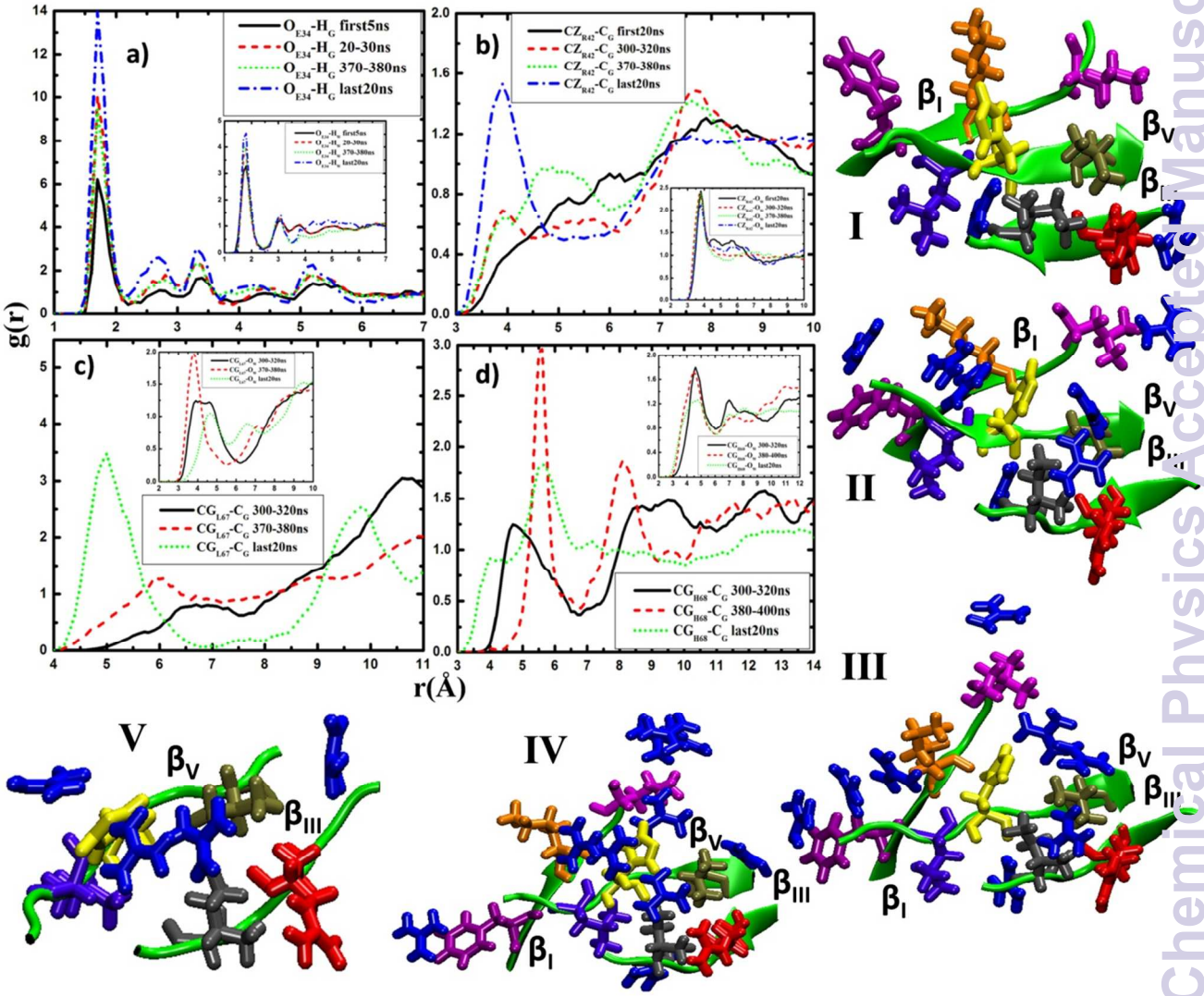

FIG. 7.

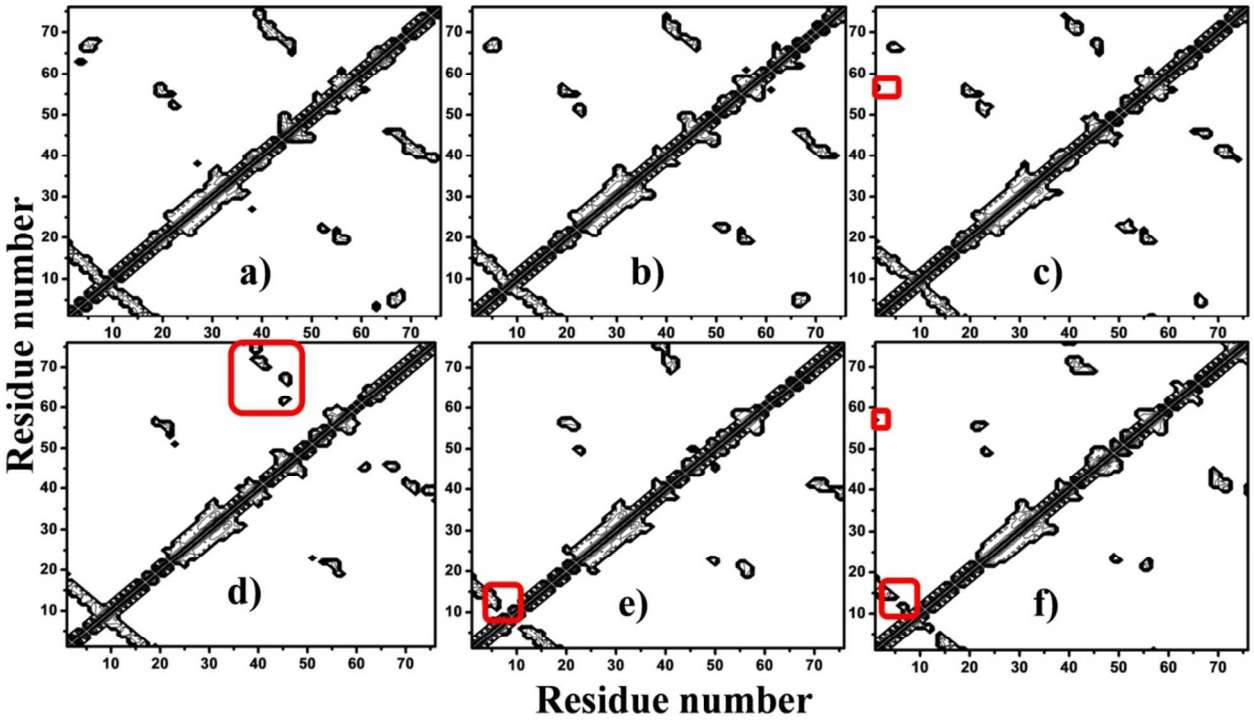

FIG. 8.

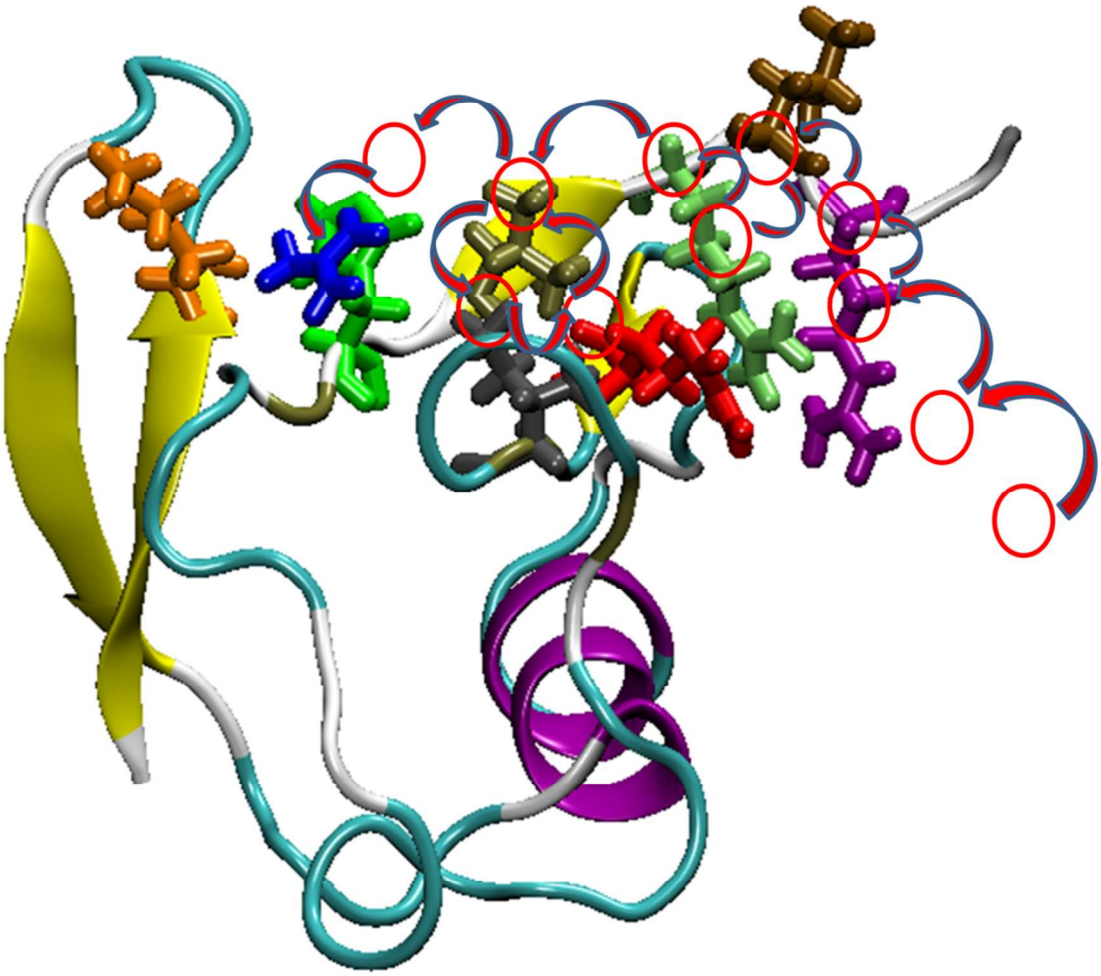

FIG. 9.

Table of Contents (TOC) Graphic

Microsecond molecular dynamics simulation of guanidinium chloride induced unfolding of ubiquitin

Manoj Mandal and Chaitali Mukhopadhyay*

Department of Chemistry, University of Calcutta

92, A.P.C. Road, Kolkata – 700 009, India

Running Title: Guanidinium chloride induced unfolding of ubiquitin.

Address for Correspondence:

Chaitali Mukhopadhyay

Department of Chemistry,

University of Calcutta,

92, A.P.C. Road, Kolkata - 700 009, India

Email : chaitalicu@yahoo.com, cmchem@caluniv.ac.in

Phone : 91-033-2351-8386

FAX : 91-033-2351-9755